The Supporting Information

for

Single-step Synthesized Functionalized Copper Carboxylate Framework Meshes as Hierarchical Catalysts for Enhanced Reduction of Nitrogen-containing Phenolic Contaminants

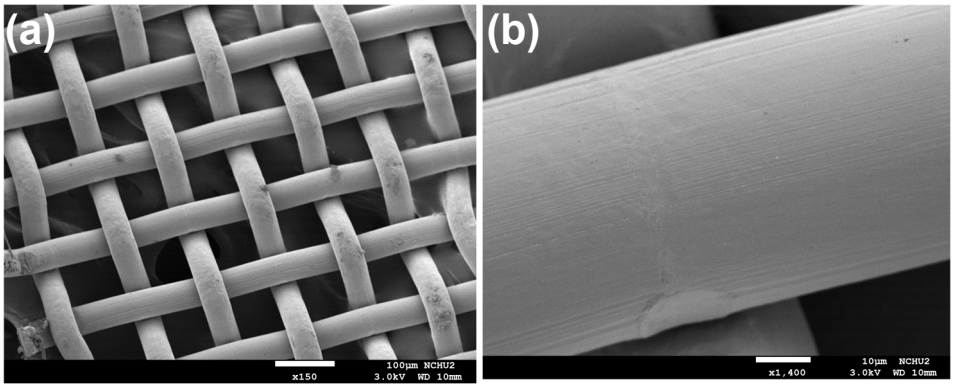

Figure S1 SEM images of the pristine Cu mesh.

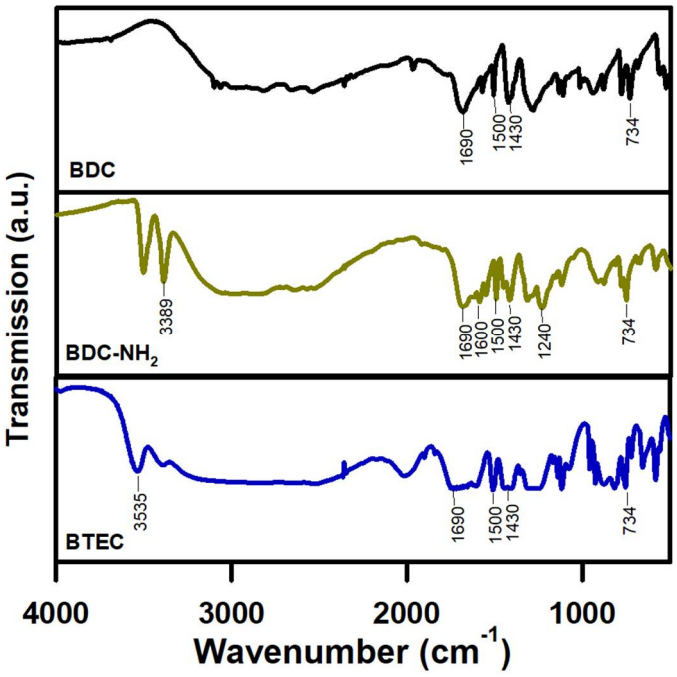

Figure S2. IR analyses of ligands.

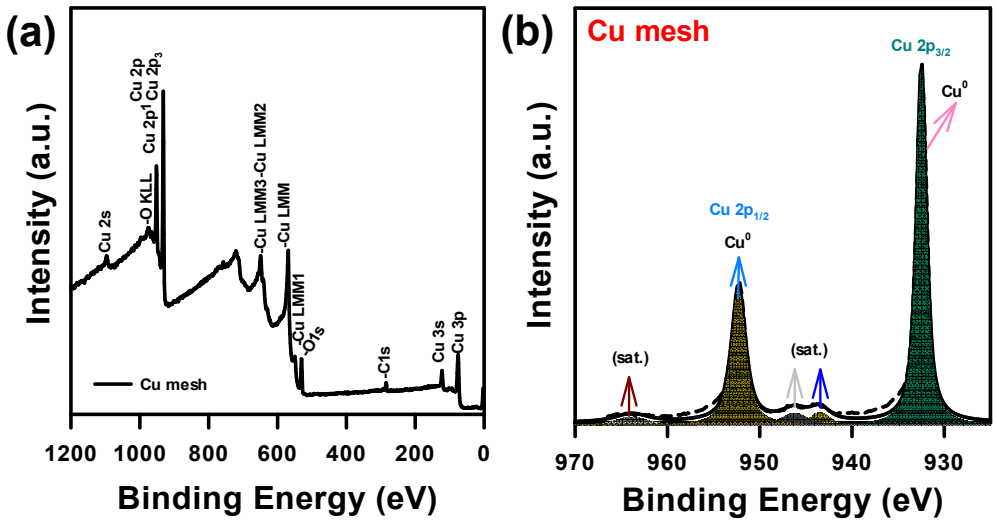

Figure S3. XPS of pristine Cu mesh: (a) full spectrum, and (b) Cu2p.

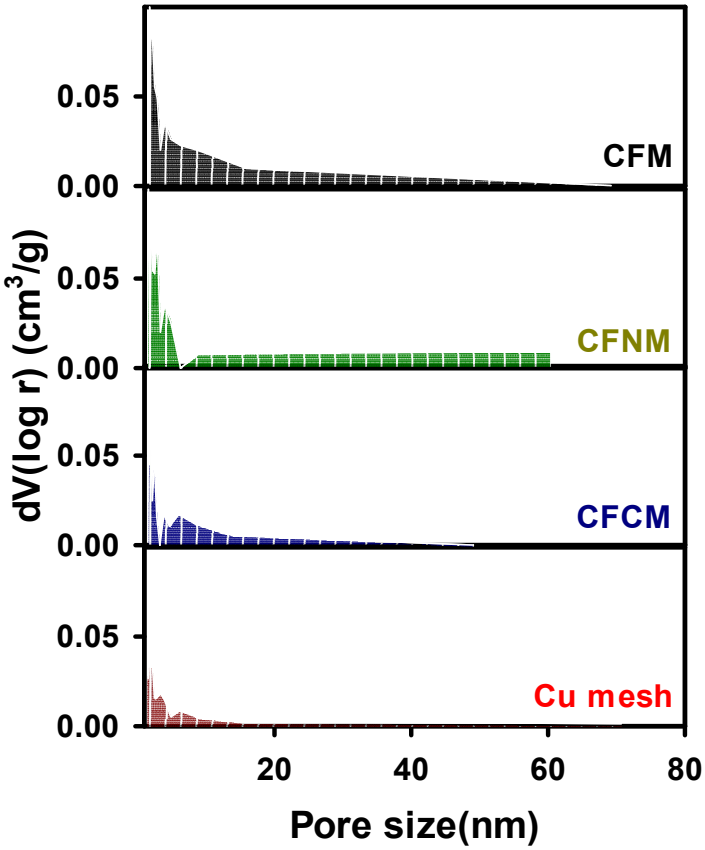

Figure S4. Pore size distributions of CF meshes.

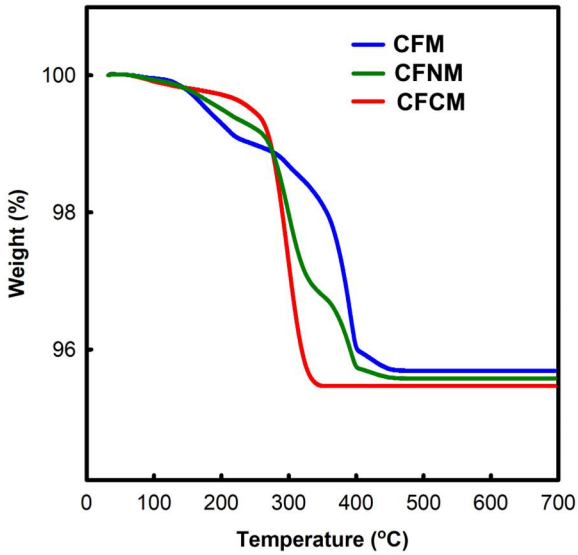

Figure S5. Thermogravimetric analyses of CuCF meshes in N_2.

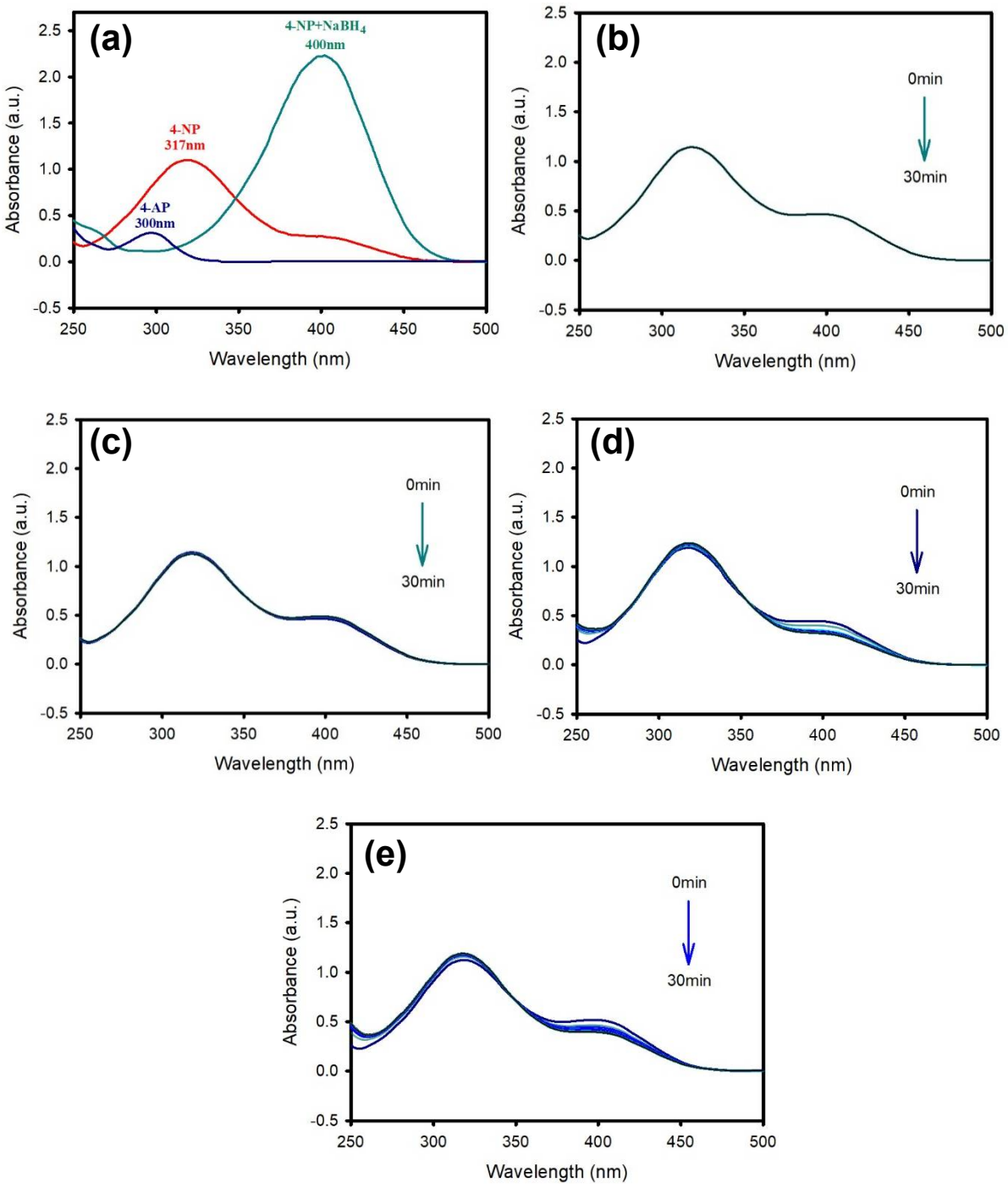

Figure S6. UV-Vis spectra of (a) 4-NP with and without $NaBH_4$, and 4-AP; (b) 4-NP (without $NaBH_4$) in the presence of pristine Cu mesh, (c) 4-NP (without $NaBH_4$) in the presence of CFM, (d) 4-NP (without $NaBH_4$) in the presence of CFNM, (e) 4-NP (without $NaBH_4$) in the presence of CFCM.

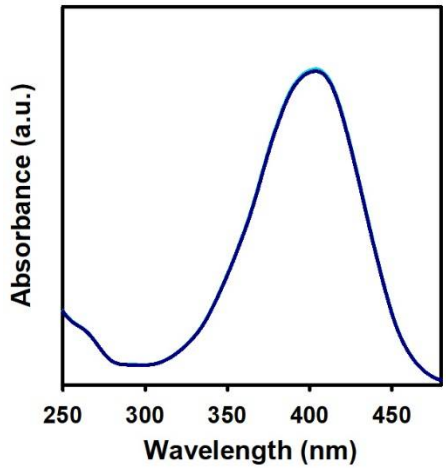

Figure S7. UV-Vis spectra of 4-NP with $NaBH_4$ in the presence of pristine Cu mesh.

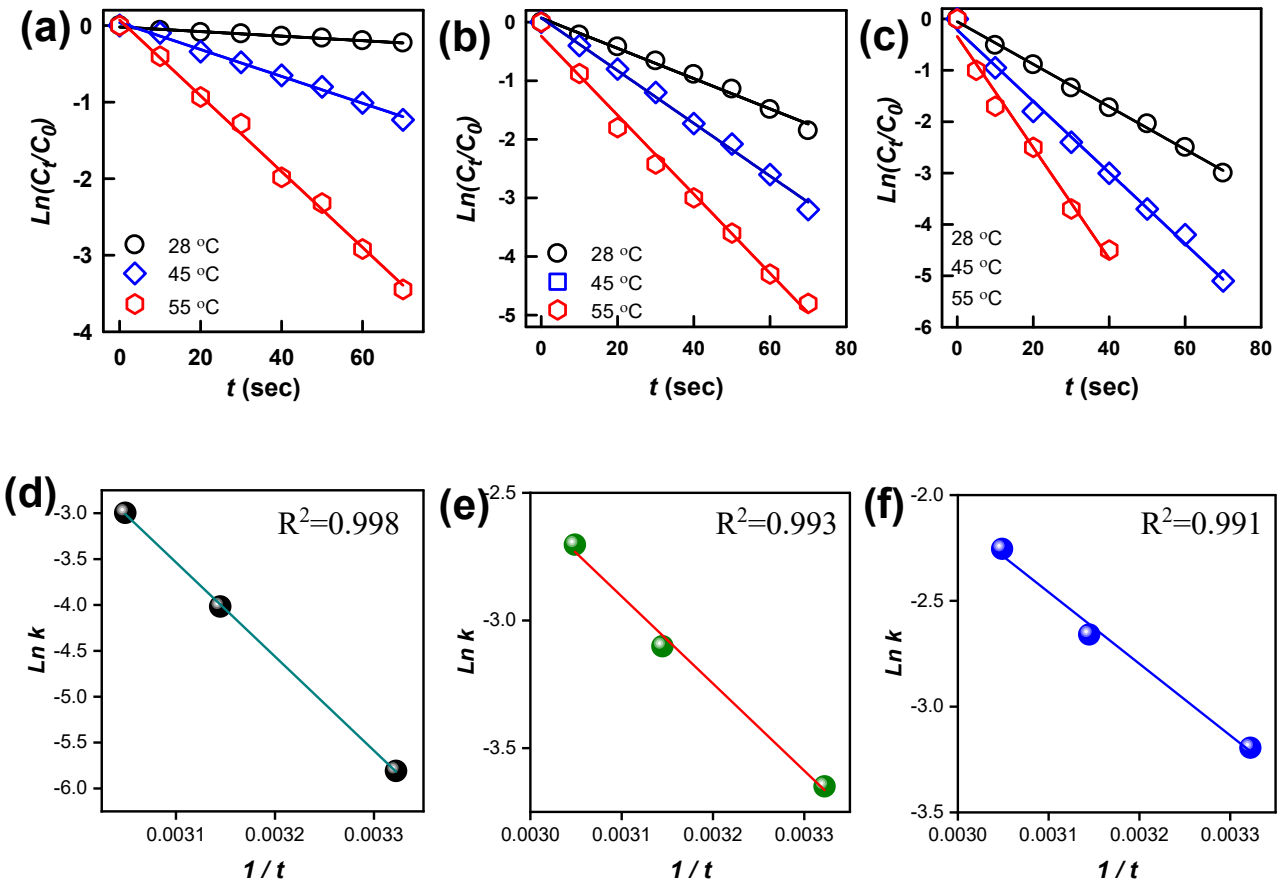

Figure S8. 4-NP reduction plots of Ln (Ct/C0) vs t, and plots of Ln K vs 1/t of by (a, d) CFM, (b, e) CFNM, and (c, f) CFCM.

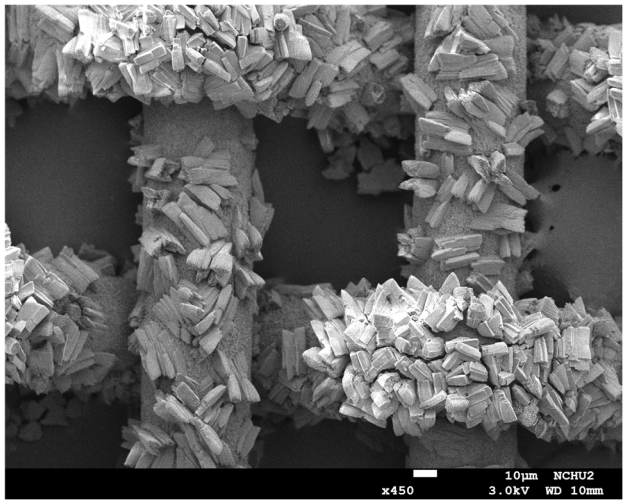

Figure S9. SEM image of the used CFCM.

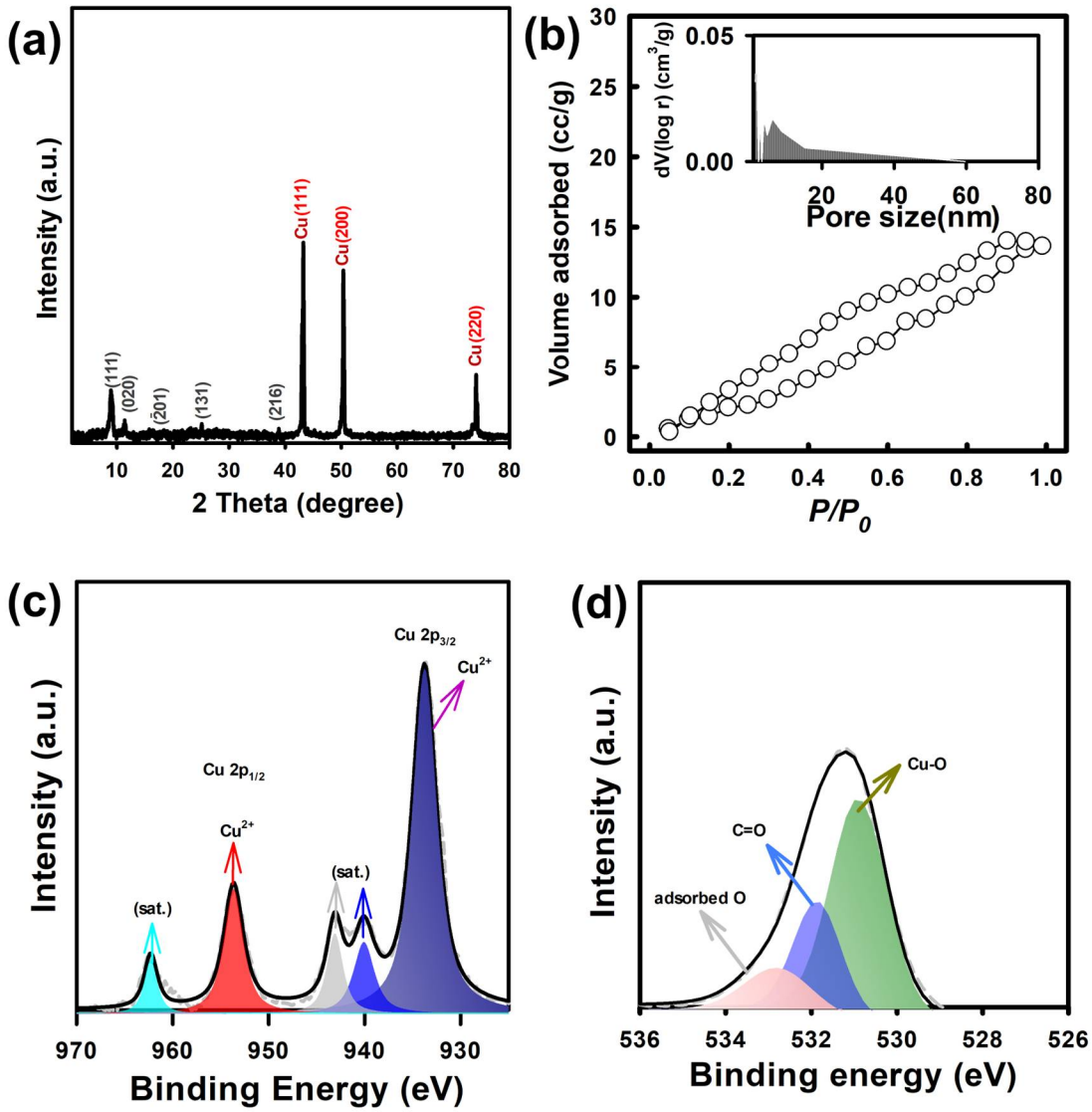

Figure S10. (a) XRD, (b) N_2 sorption isotherm, and XPS analyses of used CFCM: (c) Cu2p, and (d) O1s core-level spectra.

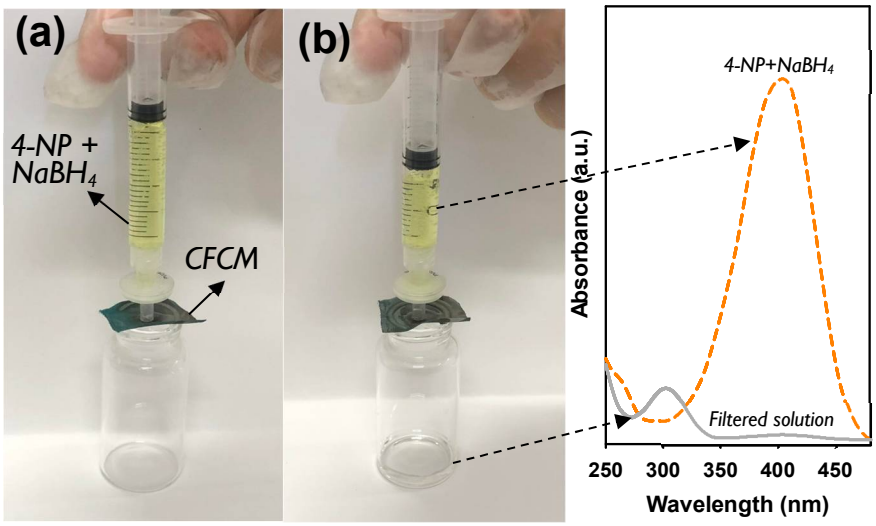

Figure S11. Demonstration of filtration-type 4-NP reduction by CFCM.

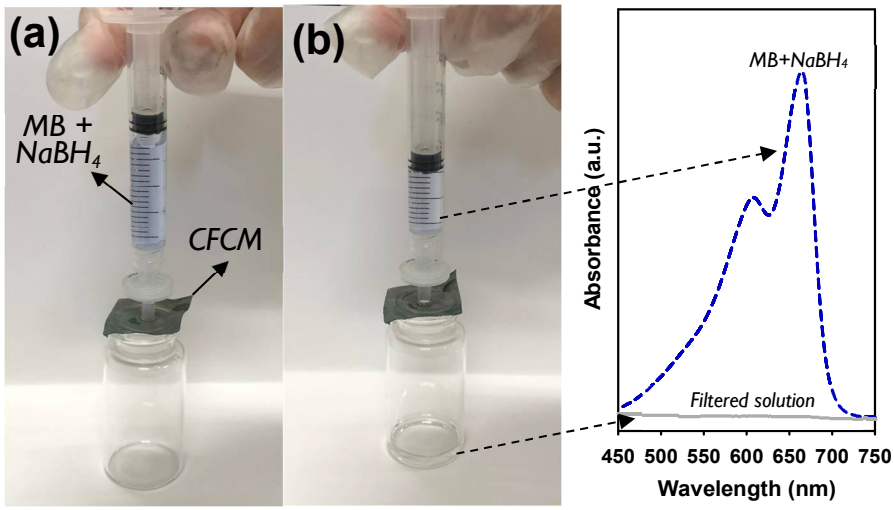

Figure S12. Demonstration of filtration-type MB reduction by CFCM.

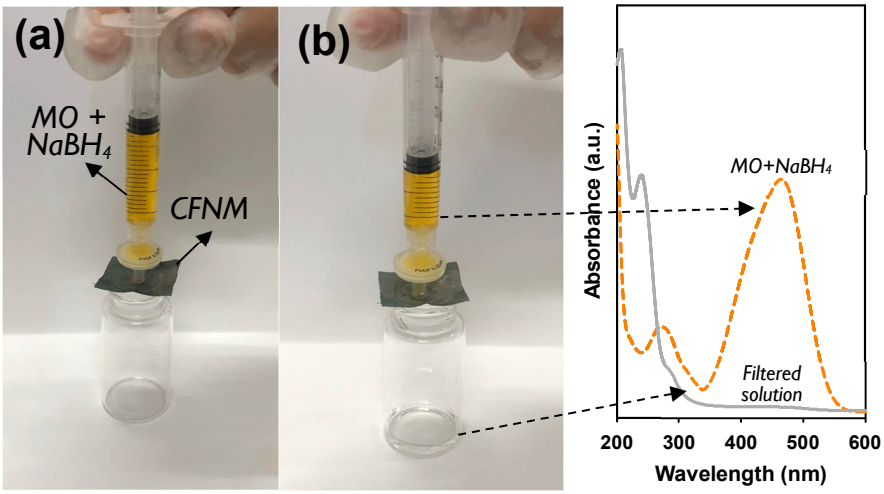

Figure S13. Demonstration of filtration-type MO reduction by CFNM.